AEM Accepts, published online ahead of print on 19 September 2014
Appl. Environ. Microbiol. doi:10.1128/AEM.02342-14
Copyright © 2014, American Society for Microbiology. All Rights Reserved.

1 **Conversion of the *Pseudomonas aeruginosa* Quinolone Signal (PQS) and Related**

2 **Alkylhydroxyquinolines by *Rhodococcus* sp. strain BG43**

3

4 Christine Müller, Franziska S. Birmes, Heiko Niewerth, and Susanne Fetzner#

5

6 Institute of Molecular Microbiology and Biotechnology, University of Münster, Münster,

7 Germany

8

9 Running Head: Degradation of the *Pseudomonas* Quinolone Signal PQS

10

11 # Address correspondence to: Susanne Fetzner, fetzner@uni-muenster.de

12

13 C.M. and F.S.B. contributed equally to this work.

AEM Accepts published online ahead of print

Downloaded from http://aem.asm.org/ on October 17, 2017 by guest

AEM Accepts published online ahead of print

14 **Abstract**

15 A bacterial strain, which based on the sequences of its 16S rRNA, *gyrB, catA* and *qsdA* genes
16 was identified as a *Rhodococcus* sp. closely related to *R. erythropolis*, was isolated from soil by
17 enrichment on PQS (the *Pseudomonas* quinolone signal, 2-heptyl-3-hydroxy-4(1*H*)-quinolone), a
18 quorum sensing signal employed by the opportunistic pathogen *Pseudomonas aeruginosa*. The
19 isolate, termed *Rhodococcus* sp. BG43, cometabolically degraded PQS as well as its biosynthetic
20 precursor 2-heptyl-4(1*H*)-quinolone (HHQ) to anthranilic acid. HHQ degradation was
21 accompanied by transient formation of PQS, and HHQ hydroxylation by cell extracts required
22 NADH, indicating that strain BG43 has a HHQ monooxygenase isofunctional to the biosynthetic
23 enzyme PqsH of *P. aeruginosa*. The enzymes catalyzing HHQ hydroxylation and PQS
24 degradation were inducible by PQS, suggesting a specific pathway. Remarkably, *Rhodococcus*
25 sp. BG43 is also capable of transforming 2-heptyl-4-hydroxyquinoline-*N*-oxide to PQS. It thus
26 converts an antibacterial secondary metabolite of *P. aeruginosa* to a quorum sensing signal
27 molecule.

28

29 **INTRODUCTION**

30 Bacteria use cell-to-cell communication systems based on chemical signal molecules to
31 coordinate their behavior within the population. These quorum sensing (QS) systems regulate a
32 variety of physiological processes, such as bioluminescence, sporulation, competence for DNA
33 uptake, biofilm maturation, production of secondary metabolites, and expression of virulence
34 factors (1). The QS network of the opportunistic pathogen *Pseudomonas aeruginosa* involves the
35 two acylhomoserine lactone (AHL)-based Las and Rhl systems, producing and responding to *N*-
36 3-oxo-dodecanoyl homoserine lactone and *N*-butanoyl homoserine lactone, respectively, and the

Downloaded from http://aem.asm.org/ on October 17, 2017 by guest

AEM Accepts published online ahead of print

37 Pqs system that is based on specific 2-*n*-alkyl-4(1*H*)-quinolones (AQ). 2-Heptyl-3-hydroxy-
38 4(1*H*)-quinolone, termed the "*Pseudomonas* quinolone signal" (PQS), is the major AQ signal in
39 *P. aeruginosa*, but its biosynthetic precursor 2-heptyl-4(1*H*)-quinolone (HHQ) also acts as a QS
40 signal molecule. PQS signaling is involved in the control of virulence factor production,
41 including the formation of elastase, pyocyanin, and lectin LecA, and it influences biofilm
42 maturation. PQS additionally has iron chelating and membrane altering properties (reviewed in
43 refs. 2−4).

44 Whereas PQS appears to be unique to *P. aeruginosa*, other *Pseudomonas* as well as
45 *Alteromonas* spp. seem to rely on non-hydroxylated 2-alkyl-4(1*H*)-quinolones, and *Burkholderia*
46 spp. use mainly 3-methylated AQs for signaling (5−8). However, *P. aeruginosa* produces more
47 than 50 AQs and related compounds (9). Among these are the 2-alkyl-4-hydroxyquinoline *N*-
48 oxides, which are close analogs of the quinones/semiquinones involved in membrane-associated
49 electron transport chains and thus act as inhibitors of respiratory cytochromes (10, 11).

50 There is considerable interest in agents that selectively interfere with the QS systems of
51 pathogenic bacteria, in order to target bacterial virulence and to develop new anti-infective
52 therapies (12). Compared with antibiotics therapy, quorum sensing interference has been thought
53 to less likely select for resistance, however, from recent studies a more varied picture emerges
54 (13, 14). Strategies to interfere with quorum sensing involve inhibition of QS signal biosynthesis,
55 inhibition of signal perception or transduction, or inactivation of the signal molecules themselves.
56 With regard to the AHLs, signal inactivation by enzymatic modification or degradation actually
57 seems to be wide-spread in nature. Some oxidoreductases catalyze the reduction of the 3-oxo
58 group of AHLs, or the ω-hydroxylation of the side chain. A wide range of Gram-negative as well
59 as Gram-positive bacteria belonging to diverse taxa, e.g., strains of *Anabaena, Agrobacterium,*

Downloaded from http://aem.asm.org/ on October 17, 2017 by guest

AEM Accepts published online ahead of print

Downloaded from http://aem.asm.org/ on October 17, 2017 by guest

60 *Pseudomonas*, *Variovorax*, *Bacillus, Arthrobacter,* and *Rhodococcus* spp., produce lactonases or
61 acylases that hydrolyze AHL signaling molecules (for recent reviews, see refs. 15, 16).

62 Rhodococci are virtually ubiquitous bacteria residing in soil and water environments.
63 They show high resistance to harsh environmental conditions such as desiccation (17, 18) and are
64 well known for their catabolic versatility. The hydrophobic cell surface containing mycolic acids
65 as well as the ability of many rhodococci to produce biosurfactants is thought to support the
66 assimilation of hydrophobic substrates by increasing their bioavailability (19, 20). Interestingly, a
67 number of *Rhodococcus* isolates can utilize AHL signal molecules as carbon source. In *R.*
68 *erythropolis* W2, *R. erythropolis* R138, and related strains, the ability to efficiently degrade
69 AHLs appears to be correlated with a conserved γ-lactone degradation pathway, with the
70 lactonase QsdA as the key enzyme (21−23). *R. erythropolis* strains possessing this pathway
71 significantly reduced tissue maceration of potato tubers by the soft-rot pathogens *Pectobacterium*
72 *carotovorum* subsp. *carotovorum* or *P. atrosepticum* (23−25).

73 Whereas numerous reports can be found in the literature on the biodegradation of AHLs,
74 bacteria that degrade AQ-type signaling molecules have not been described so far. The only
75 enzyme known to be able to inactivate an AQ-type QS signal is the dioxygenase Hod (1*H*-3-
76 hydroxy-4-oxoquinaldine 2,4-dioxygenase) from *Arthrobacter* sp. Rue61a, which catalyzes the
77 cleavage of PQS to form *N*-octanoylanthranilate and carbon monoxide (26). However, Hod is an
78 enzyme involved in the 2-methylquinoline degradation pathway of *Arthrobacter* sp. Rue61a, with
79 3-hydroxy-2-methyl-4(1*H*)-quinolone (MHOQ) as its physiological substrate (27, 28), and its
80 comparatively low activity towards PQS is considered as fortuitous.

81 Quinoline and quinolone alkaloids structurally related to the AQ-type signaling molecules
82 of *P. aeruginosa* and *Burkholderia* spp. are produced by a variety of higher organisms, especially

AEM Accepts published online ahead of print

83 by plants of the family *Rutaceae* (2, 29, 30). Therefore, it is well conceivable that soil
84 microorganisms have evolved enzymes and pathways to detoxify and/or to degrade quinolones.
85 In this study, we isolated a PQS-degrading bacterium from soil. The isolate was identified as a
86 *Rhodococcus* strain related to the species *R. erythropolis*. It cometabolically degrades PQS to
87 anthranilic acid, and it is also able to convert the PQS precursor HHQ as well as related 2-alkyl-
88 4-hydroxyquinolines of *P. aeruginosa*.

89

90 **MATERIALS AND METHODS**

91 **Chemicals.** HHQ and 2-heptyl-4-hydroxyquinoline *N*-oxide (HQNO) were produced by *P.*
92 *putida* KT2440 [pBBR-*pqsABCD*] and *P. putida* KT2440 [pBBR-*pqsABCD*; pME6032-*pqsL*],
93 respectively, grown in the presence of anthranilate and octanoate, and isolated from biomass as
94 described previously for AQs (31). HHQ extracts which were not purified further by preparative
95 HPLC also contained minor amounts of other AQs with C_9–C_{13} saturated and unsaturated alkyl
96 side chains. HQNO was purified by preparative HPLC (31). For *in vitro* assays and as reference
97 compound, HQNO purchased from Enzo Life Sciences was used. 3-Hydroxy-2-methyl-4(1*H*)-
98 quinolone (MHOQ) was synthesized from 3-formyl-2-methyl-4(1*H*)-quinolone (32, 33). PQS, *N*-
99 acetylanthranilic acid and anthranilic acid were from Sigma-Aldrich. Stock solutions of PQS,
100 HHQ and HQNO were prepared in methanol. MHOQ and *N*-acetylanthranilic acid were
101 dissolved in ethanol and deionized water, respectively.

102 **Isolation of a PQS-degrading bacterial strain.** Soil samples, collected in the botanical
103 garden of the University of Münster beneath plants that produce quinoline or acridone alkaloids
104 (*Ephedra spp., Ruta graveolens, Ptelea trifoliata, Citrus limon, Citrus aurantium*, *Poncirus*
105 *trifoliata*), as well as soil samples collected below spruce, oak and beech trees in forests in the
106 Münster area and soil collected at a roadside were shaken for 1 h in 0.9% (wt/vol) NaCl solution.

Downloaded from http://aem.asm.org/ on October 17, 2017 by guest

AEM Accepts published online ahead of print

Downloaded from http://aem.asm.org/ on October 17, 2017 by guest

107 The suspensions were used to inoculate 24-well microtiter plates (CELLSTAR Suspension
108 Culture Plates, Greiner Bio-One GmbH) containing mineral salts medium (6.78 g/l
109 $Na_2HPO_4 \times 2H_2O$; 3 g/l KH_2PO_4; 0.5 g/l NaCl; 1 g/l NH_4Cl; 2 mM $MgSO_4$; 0.1 mM $CaCl_2$; 15
110 mg/l $Na_2MoO_4 \times 7H_2O$; 1 ml/l trace element solution (34), supplemented with 50 µM PQS as sole
111 carbon source. Culture samples were diluted into fresh medium every week for six times, even
112 though growth or biofilm formation was hardly (if at all) detectable. Samples taken from the last
113 transfer were spread onto Luria-Bertani agar plates (LB, 35). Colonies were purified by repeated
114 alternate streaking on agar plates containing PQS mineral salts medium and LB agar. Individual
115 isolates were tested for cometabolic PQS conversion as described below.

116 **Bacterial strains and growth conditions.** *Rhodococcus* sp. BG43 as well as *P. putida*
117 KT2440 [pBBR-*pqsABCD*], *P. putida* KT2440 [pBBR-*pqsABCD*; pME6032-*pqsL*] and *E. coli*
118 DH5α [pME6032-*pqsL*] were grown in LB medium at 30°C and 37°C, respectively. 50 µg/ml
119 kanamycin and 50 µg/ml tetracycline were added to cultures of recombinant *P. putida* KT2440,
120 and 12.5 µg/ml tetracycline to recombinant *E. coli* DH5α cultures. To determine growth of
121 *Rhodococcus* sp. BG43 on individual carbon or nitrogen sources, cells of overnight LB cultures
122 were pelleted by centrifugation (8000 × *g*, 5 min, 4°C), washed twice with phosphate buffered
123 saline (PBS), and used to inoculate modified KG medium to an optical density at 600 nm
124 (OD_{600nm}) of 0.05. The modified KG medium (36) contains 1.25 g/l NaCl, 0.75 g/l KCl, 0.25 g/l
125 Na_2SO_4, 0.25 g/l KH_2PO_4 and 1.0 g/l 2-(*N*-morpholino)-ethanesulfonic acid (MES). The pH was
126 adjusted to 6.5, and after autoclaving, the following components were added from sterile stock
127 solutions: 0.5 ml/l vitamin solution (37), NH_4Cl (0.3 g/l), $MgCl_2$ (0.5 g/l), $CaCl_2$ (0.25 g/l), $FeCl_3$
128 (5 mg/l), and $MnCl_2$ (2.5 mg/l). For testing the utilization of substrates as nitrogen source, NH_4Cl
129 was omitted from the medium and 1% (wt/vol) succinate was used as carbon source. For all
130 growth tests, cultures lacking the substrate to be tested were run in parallel. Strain BG43 did not

131 grow in the MES-buffered medium in the absence of another substrate. The cultures were
132 incubated at 30°C on a rotary shaker (160 rpm), and OD_{600nm} was measured within 24 h.

133 The viability of cell suspensions of *Rhodococcus* sp. strain BG43 in modified KG medium
134 with succinate, supplemented with up to 20 µM HQNO, was monitored with the BacTiter-Glo™
135 Microbial Cell Viability Assay (Promega Corporation), which quantifies ATP levels as an
136 indicator for metabolically active cells. Cell suspensions were set up as performed for the AQ
137 conversion assays (see below), i.e., strain BG43 was suspended in the medium to an initial
138 OD_{600nm} of 3. Samples were taken at different time points within 4 h and frozen immediately. The
139 BacTiter-Glo assay was prepared in multiwell plates as described by the manufacturer, using
140 series of diluted samples. Antibacterial activity of HQNO towards strain BG43 was tested by
141 growing the strain in modified KG medium with succinate in the presence of up to 500 µM
142 HQNO. Cultures were incubated at 30°C on a rotary shaker and OD_{600nm} was determined.

143 **DNA techniques.** Genomic DNA of *Rhodococcus* sp. BG43 was extracted with the
144 innuSPEED Bacteria/Fungi DNA Kit (Analytik Jena AG). PCR was performed using Q5® Hot
145 Start High-Fidelity DNA Polymerase (New England Biolabs GmbH). Plasmids and PCR
146 products were purified with the innuPREP Plasmid Mini Kit and innuPREP DOUBLEpure Kit
147 (Analytik Jena AG), respectively. Agarose gel electrophoresis, restriction and ligation were
148 performed using standard protocols (35). Restriction enzymes were purchased from Thermo
149 Scientific. For transformation of *E. coli* DH5α, cells were prepared according to the method of
150 Hanahan (38). Oligonucleotides were purchased from Eurofins MWG Operon. DNA sequencing
151 was carried out by GATC Biotech AG.

152 **Construction of pME6032-*pqsL*.** The *pqsL* gene (nt 4687652-4688848, NC_002516) of
153 *P. aeruginosa* PAO1 (University of Nottingham strain) was amplified using the primer set pqsL-
154 for/pqsL-rev (Table 1). The PCR product, digested with *Eco*RI and *Sac*I, was ligated into the

AEM Accepts published online ahead of print

Downloaded from http://aem.asm.org/ on October 17, 2017 by guest

AEM Accepts published online ahead of print

155 appropriately digested plasmid pME6032 (40), and *E. coli* DH5α was transformed with the
156 pME6032-*pqsL* plasmid. To generate a HQNO producing strain, *P. putida* KT2440 [pBBR-
157 *pqsABCD*] (31) was transformed with pME6032-*pqsL* by electroporation essentially as described
158 in ref. (39), with the following electrical settings: voltage 12.5 kV/cm; capacitor: 25 µF, resistor:
159 200 Ω. After discharge, 400 µl of LB medium was added, and the cell suspension was incubated
160 for 1 h at 30 °C with shaking before plating on selective media.

161 **Molecular characterization and phylogenetic analysis of strain BG43.** To classify the
162 PQS-converting isolate, the gene encoding 16S ribosomal RNA as well as genes coding for
163 catechol 1,2-dioxygenase (*catA*) and gyrase B (*gyrB*) were amplified using the primer pairs
164 GM3F/GM4R, catA-for/catA-rev, and gyrB-for/gyrB-rev, respectively (41−43) (Table 1).
165 Phylogenetic trees generated from the 16S rDNA, *catA* and *gyrB* sequences using the Neighbor-
166 Joining algorithm were constructed with the Molecular Evolution Genetics Analysis (MEGA)
167 software version 6.0 (44). Nucleotide alignment was carried out with MUSCLE (45). The
168 reliability of the trees was evaluated by bootstrap analysis (1000 resamplings). The *qsdA* gene
169 encoding a "*Rhodococcus*-specific" AHL lactonase (21) was amplified with the primers qsdA-for
170 and qsdA-rev (46) (Table 1).

171 **Preparation of cell extracts.** For preparation of crude cell extracts, *Rhodococcus* sp.
172 BG43 was cultivated in LB medium for 24 h under vigorous shaking. To possibly induce the
173 expression of genes of an AQ degradation pathway, 20 µM PQS was added 2 h before cells were
174 harvested by centrifugation (12,000 × *g*, 4°C, 45 min). Cells resuspended in 50 mM potassium
175 phosphate buffer (pH 7.5) were disrupted by sonication at 4°C. Cell-free crude extracts
176 containing soluble proteins were obtained by centrifugation for 40 min at 38,360 × *g* and 4°C.
177 For removal of salts and small molecules, Zeba Spin Desalting Columns (7000 molecular weight

Downloaded from http://aem.asm.org/ on October 17, 2017 by guest

AEM Accepts published online ahead of print

178 cutoff, Thermo Scientific) were used. The method of Bradford as modified by Zor and Selinger
179 (47) was applied to estimate the protein concentration. Bovine serum albumin served as a
180 standard protein.

181 **AQ conversion by whole cells and crude cell extracts.** Cells of *Rhodococcus* sp. BG43
182 cultures grown for 24 h in LB medium were pelleted by centrifugation (9,000 × *g*, 4°C, 10 min)
183 and washed twice with PBS. Subsequently the cells were resuspended in modified KG medium
184 containing 1% (wt/vol) succinate as carbon source, and diluted to an OD_{600nm} of 3. After addition
185 of 20 µM MHOQ, HHQ, PQS, or HQNO, the cultures were incubated at 30°C with constant
186 shaking. Cultures without added AQ were run in parallel. Samples (25 ml cell suspension) were
187 taken at different time points, and AQs were extracted as described below. For measuring AQ
188 conversion by desalted crude cell extracts, the protein concentration of the extracts was set to 2 or
189 1 mg/ml. When indicated, NADH or NADPH, with or without additional 500 µM FAD, were
190 added to a final concentration of 500 µM. Sets of test tubes containing 1 ml aliquots were
191 supplemented with 20 µM PQS, HHQ, or HQNO, and incubated at 30°C with shaking at 900
192 rpm. Test tubes were sacrificed at different time points for extraction with ethyl acetate.

193 **Extraction of AQs.** Prior to extraction with ethyl acetate, samples were spiked with 1 µM
194 *N*-acetylanthranilic acid in order to monitor the reproducibility of sample extraction. Samples of
195 *Rhodococcus* sp. BG43 cultures incubated with AQs (25 ml each) and crude cell extract samples
196 (1 ml each) were extracted with 3 × 5 ml and 3 × 0.5 ml, respectively, of acidified ethyl acetate (1
197 ml acetic acid/l). After centrifugation at 9,000 × *g* for 5 min and 20,000 × *g* for 5 min,
198 respectively, the organic phases of each sample were combined, dried to completion, and the
199 residue was re-dissolved in methanol. Using this protocol, about 86%, 79%, 65%, 21%, and 80%

Downloaded from http://aem.asm.org/ on October 17, 2017 by guest

AEM Accepts published online ahead of print

200 of HHQ, PQS, HQNO, MHOQ, and anthranilic acid, respectively, could be recovered from 20
201 µM solutions in modified KG medium.

202 **Analytical methods.** HPLC was performed on a 250 × 4 mm Eurospher II RP-18 column
203 at 35°C. Extracts containing PQS or HQNO and extracts of negative controls without AQs were
204 separated using a linear gradient (20 min) of 80% (vol/vol) methanol in water to 100% methanol,
205 at a flow rate of 0.5 ml/min. For analysis of extracts containing HHQ or MHOQ, a linear gradient
206 (40 min) of 15% (vol/vol) methanol in water to 100% methanol was applied at a flow rate of 0.5
207 ml/min. All eluents were acidified with 1 g/l citric acid. Light absorption spectra were recorded
208 with a diode array detector (L-2450 LaChrome Elite®, Merck Hitachi). Reference compounds
209 were used to calibrate the column for quantitative determination of AQs. Intermediates of AQ
210 transformation were analyzed by liquid chromatography-mass spectrometry on a Dionex™
211 Ultimate™ 3000 UHPLC system (Thermo Scientific), coupled with an electrospray ionization
212 ion trap mass spectrometer (amaZon Speed, Bruker Daltonics), using a scan range from 50 to
213 1000 *m/z* (target mass 300 *m/z*). The capillary voltage was set to 4000 V and the capillary
214 temperature to 200°C.

215 **Accession numbers.** The (partial) sequences of the 16S rRNA gene and the *catA*, *qsdA*,
216 and *gyrB* genes obtained in this study were deposited in the GenBank nucleotide sequence
217 database under accession numbers KM093741, KM093742, KM093743 and KM093744,
218 respectively.

219

220 **RESULTS**

221 **Isolation of the PQS-converting strain BG43.** Enrichment cultures were established in
222 mineral salts medium containing the QS signal molecule PQS as carbon source using soil

Downloaded from http://aem.asm.org/ on October 17, 2017 by guest

AEM Accepts published online ahead of print

223 samples as inocula. Purification of bacterial colonies by repeated alternate streaking on PQS
224 mineral salts agar and LB agar plates resulted in 8 isolates, all from soil samples of the botanical
225 garden of the University of Münster. When tested for cometabolic PQS biotransformation in
226 modified KG medium supplemented with succinate, seven out of the eight isolates showed
227 tolerance towards PQS rather than PQS degradation. One isolate, termed strain BG43, which
228 transforms PQS as described below, originated from soil collected below *Ruta* and *Ephedra*
229 plants. Apparently, the protocol used for sub-culturing of the enrichment cultures and strain
230 isolation predominantly selected for bacteria able to survive comparatively high concentrations of
231 PQS and extended periods of starvation.

232 **Phylogenetic analysis and carbon source utilization pattern of strain BG43.** BLASTn
233 analysis (Standard Nucleotide Blast; http://blast.st-va.ncbi.nlm.nih.gov/Blast.cgi) of the partial
234 sequence (1359 nt) of the 16S rRNA gene of strain BG43 revealed highest levels of sequence
235 identity to 16S RNA genes of *R. erythropolis* strains zzx26, D7 and WZ010 (99.78%). The
236 highest level of sequence identities to type strains occurred with *R. qingshengii* strain djl-6 (DSM
237 45222^T) (99.71%). The phylogenetic tree based on the 16S rRNA gene sequences of
238 *Rhodococcus* sp. BG43 and type strains of other *Rhodococcus* species supports a close
239 relatedness to *R. qingshengii* DSM 45222^T and *R. erythropolis* DSM 43066^T (Fig. 1A). Since the
240 identities among the partial 16S rRNA gene sequences were very high, additionally the sequences
241 of PCR products of the *gyrB* and *catA* genes, which have been used as marker genes for
242 *Rhodococcus* (43), were compared to those of *Rhodococcus* type species. The phylogenetic tree
243 based on *gyrB* sequences suggested that strain BG43 and *R. erythropolis* DSM 43066^T are closely
244 related (Fig. 1B), whereas analysis of *catA* led to a tree clustering the isolate with *R. qingshengii*
245 DSM 45222^T (Fig. 1C). However, a phylogenetic tree based on the concatenated sequences
246 places strain BG43 closer to the *R. erythropolis* type strain (Fig. 1D).

Downloaded from http://aem.asm.org/ on October 17, 2017 by guest

247 A comparison of the carbon source utilization patterns of strain BG43 and related 248 *Rhodococcus* type species (48, 49) (Table 2) shows that all strains are able to utilize glycerol but 249 not lactose. Even though the *catA* gene encoding catechol 1,2-dioxygenase is present in the 250 genome of *Rhodococcus* sp. BG43, it did not grow on catechol under the conditions tested, as 251 also observed for some other *Rhodococcus* sp. strains. In contrast to *R. qingshengii* DSM 45222^T, 252 *R. globerulus* DSM 43954^T and *R. baikonurensis* DSM 44587^T, *Rhodococcus* sp. BG43 is able to 253 grow on *myo*-inositol, as reported for *R. erythropolis* DSM 43066^T. In contrast to *R. qingshengii* 254 DSM 45222^T, strain BG43 can utilize D-sorbitol. Taken together, the comparison of the marker 255 genes tested and the carbon source utilization patterns support the hypothesis that strain BG43 256 clusters with *R. erythropolis*, however, more detailed analyses will be required for species 257 allocation.

258 Since the AHL lactonase QsdA, a member of the phosphotriesterase (PTE) family, has 259 been identified in all out of six *R. erythropolis* strains tested (21), we speculated that strain BG43 260 might also contain this quorum quenching enzyme. PCR amplification indeed resulted in a 261 specific product, whose deduced amino acid sequence (292 aa) shows 99% identity to the 262 corresponding region (aa 18-309) of QsdA of *R. erythropolis* strain SQ1. Concordant with other 263 QsdA enzymes from *Rhodococcus* spp., the protein sequence of $QsdA_{BG43}$ diverges from the 264 consensus PTE zinc domain sequence. The sequence of motif 2 of the zinc binding site of 265 $QsdA_{BG43}$ ($\underline{A}$VGQ$\underline{A}$QVET$\underline{G}$V$\underline{P}$ITV$\underline{H}$; conserved residues of the zinc binding domain CD2 of 266 PTEs are underlined) corresponds to the allele A1 as defined by Uroz *et al.* (21), with a 267 conserved alanine at position 5 of the motif, whereas another group of rhodococcal QsdAs (allele 268 A2) has a serine at this position. Consistent with the role of QsdA as a key enzyme in the γ- 269 lactone catabolic pathway, strain BG43 was capable of growing on γ-octalactone (4.5 mM) as

AEM Accepts published online ahead of print

Downloaded from http://aem.asm.org/ on October 17, 2017 by guest

AEM Accepts published online ahead of print

270 source of carbon and energy, but not on γ-butyrolactone (9 mM, 4.5 mM, or 1 mM), as described
271 for *R. erythropolis* R138 (22).

272 **Cometabolic degradation of PQS, HHQ, and MHOQ.** Cell suspensions of
273 *Rhodococcus* sp. BG43 (OD_{600nm} ~ 3), incubated in modified KG medium with succinate,
274 transformed 20 µM of PQS within 30 min. PQS conversion was accompanied by formation of an
275 intermediate which showed the same HPLC elution behavior, UV spectrum, and fluorescent
276 properties as authentic anthranilic acid. It accumulated in the culture and was only slowly
277 degraded further (Fig. 2A). When anthranilic acid (0.5 mM) was the only carbon source in
278 modified KG medium, growth of *Rhodococcus* sp. BG43 was not observed. However, it
279 supported growth ($OD_{600\ nm}$ of 0.5 after 24 hours) when present as sole source of nitrogen.

280 MHOQ, the substrate of 1*H*-3-hydroxy-4-oxoquinaldine 2,4-dioxygenase (Hod) of
281 *Arthrobacter* sp. Rue61a (26–28), is very slowly converted by cell suspensions of strain BG43.
282 After 2 and 3 h of incubation, about 50% and 90% of the MHOQ were consumed. Only trace
283 amounts (below 0.1 µM) of anthranilic acid were detected in the cultures during MHOQ
284 conversion.

285 Cell suspensions of strain BG43 were also able to cometabolically degrade the HHQ
286 signaling molecule. Besides anthranilic acid, PQS was formed at low concentrations during HHQ
287 conversion (Fig. 2B). In cultures without any AQ addition, anthranilic acid was not detected (data
288 not shown). Interestingly, other AQ congeners, which were present in the HHQ extracted from
289 biomass of *P. putida* KT2440 [pBBR-*pqsABCD*], were also consumed by cell suspensions of
290 strain BG43 (Fig. 2C).

291 **Conversion of PQS and HHQ by crude cell extracts.** To get an indication of whether
292 the AQ degradation pathway is inducible, we compared the rates of AQ conversion by crude
293 extracts from *Rhodococcus* sp. BG43 cells grown in LB and extracts from LB-grown cells that

Downloaded from http://aem.asm.org/ on October 17, 2017 by guest

AEM Accepts published online ahead of print

294 were incubated with PQS for 2 h prior to harvesting. As illustrated in Fig. 3, desalted extracts of
295 PQS-induced cells converted HHQ as well as PQS faster than extracts from non-induced cells.
296 PQS conversion to anthranilic acid occurred in the absence of added co-substrates, whereas HHQ
297 conversion required the addition of NADH. As also observed in the *in vivo* assays (Fig. 2B),
298 HHQ turnover by cell extracts was accompanied by transient formation of PQS (data not shown).
299 When NADH was replaced by NADPH, about 85% of the initial HHQ was still present in the
300 assays after 7 h of incubation, suggesting that the HHQ monooxygenase has a high specificity for
301 NADH. The additional presence of FAD as possible mediator did neither affect the rate of
302 NADH-dependent HHQ turnover, nor support HHQ conversion in presence of NADPH.

303 **Conversion of HQNO.** The viability of strain BG43 in the presence of the quinone
304 oxidoreductase inhibitor HQNO was assessed by monitoring ATP levels in the cultures by
305 measuring luminescence in the BacTiter-Glo assay. When cell suspensions of strain BG43 were
306 cultured in modified KG medium with succinate and in the presence of 20 µM HQNO for 4 h, the
307 luminescence intensities of culture samples were in the same range as those of control cultures
308 without HQNO, suggesting that HQNO at the concentration tested does not affect cell viability.
309 Growth assays performed in modified KG medium with succinate indicated that 20 µM HQNO
310 led to slight growth retardation, which was more pronounced in the presence of 100 µM HQNO.
311 However, after cultivation for 24 h, similar optical densities were reached in cultures
312 supplemented with up to 100 µM HQNO and cultures without HQNO. Growth of strain BG43
313 was fully inhibited by 300 µM HQNO.

314 Remarkably, cell suspensions of *Rhodococcus* sp. BG4, pre-grown in LB and incubated in
315 modified KG medium under the same conditions as used in the PQS and HHQ biotransformation
316 assays with 20 µM of HQNO, were capable of cometabolically converting the *N*-oxide. HQNO
317 was very slowly transformed to PQS (Fig. 4A), identified by HPLC-MS which revealed an *m/z* of

Downloaded from http://aem.asm.org/ on October 17, 2017 by guest

318 260.14 (for [$C_{16}H_{21}NO_2 + H^+$]). The HPLC retention time and UV spectrum also were identical to
319 those of the authentic PQS reference compound. Minor amounts of a compound which based on
320 its *m/z* of 276.16 (for [$C_{16}H_{21}NO_3 + H^+$]) was identified as a hydroxylated form of HQNO were
321 also detected in the culture extracts (Fig. 4); the UV spectrum of the compound (Fig. 4B)
322 supports the assignment as an AQ congener. However, anthranilic acid was not detected in the
323 extracts.
324 When desalted crude cell extracts of LB-grown, PQS-induced cells were incubated with
325 20 µM HQNO and 500 µM NADH, trace amounts of HHQ were detected already after 5 min.
326 After 2 h of incubation, PQS was found in µM concentrations (up to 9 µM) in ethyl acetate
327 extracts of the *in vitro* assays, whilst HHQ was no longer present. Again, anthranilic acid was not
328 detected, and the HPLC elution profiles showed a minor peak of hydroxy-HQNO. NADPH did
329 not support HQNO conversion by the cell extracts. The data indicate that *Rhodococcus* sp. strain
330 BG43 detoxifies HQNO by *N*-oxide reduction and hydroxylation.
331 To assess whether the apparent accumulation of PQS from HQNO was due to direct
332 inhibition or inactivation of the PQS-converting enzyme by HQNO or a metabolite thereof,
333 desalted crude cell extracts of PQS-induced cells were pre-incubated with NADH and 0, 20 or 50
334 µM HQNO, and subsequently PQS was added to each sample. Since the kinetics of anthranilate
335 formation from PQS were not affected by the presence of HQNO (Fig. 5), there is no indication
336 of enzyme inhibition.
337
338 **DISCUSSION**
339 The soil isolate *Rhodococcus* sp. strain BG43 is capable of degrading the *P. aeruginosa* quorum
340 sensing signaling molecules HHQ and PQS to anthranilic acid (Fig. 6). The $C_{7:1}$ unsaturated
341 congener of HHQ as well as AQs with C_9- and C_{11}- saturated and unsaturated alkyl chains were

AEM Accepts published online ahead of print

Downloaded from http://aem.asm.org/ on October 17, 2017 by guest

AEM Accepts published online ahead of print

342 also converted. Cell extracts of strain BG43 containing the soluble (cytoplasmic) proteins
343 hydroxylated HHQ to PQS in an NADH-dependent reaction, suggesting that strain BG43
344 produces a monooxygenase that is isofunctional to the HHQ 3-monooxygenase PqsH of *P.*
345 *aeruginosa*, which catalyzes the terminal step in PQS biosynthesis (50). PQS conversion to
346 anthranilic acid by desalted crude cell extracts was independent of added cosubstrates. The steps
347 involved remain to be biochemically characterized, however, it is conceivable that they proceed
348 analogous to the conversion of MHOQ in the 2-methylquinoline degradation pathway of
349 *Arthrobacter* sp. Rue61a. In this pathway, the intermediate MHOQ undergoes a dioxygenase-
350 catalyzed ring cleavage to carbon monoxide and *N*-acetylanthranilic acid, followed by amide
351 hydrolysis to anthranilic acid and acetate (27).

352 MHOQ, the physiological substrate of the dioxygenase Hod, which has weak activity
353 towards PQS (26), was also transformed by cell suspensions of *Rhodococcus* sp. BG43, but
354 significantly more slowly than PQS. Assuming that the same enzymes of strain BG43 catalyze
355 the conversion of MHOQ and PQS, they are more specific for PQS. Moreover, in *Rhodococcus*
356 sp. BG43 the pathway of HHQ degradation via PQS appears to be PQS-inducible, supporting the
357 hypothesis of AQ-specific rather than fortuitous reactions.

358 The *Rhodococcus* sp. strain BG43 was isolated from soil collected beneath plants that are
359 known to synthesize quinoline alkaloids. *Ruta graveolens*, for example, produces 2-*n*-nonyl-
360 4(1*H*)-quinolone besides other 4(1*H*)-quinolones (29). Since HHQ and PQS hardly support
361 growth of strain BG43, induction of AQ bioconversion by PQS might suggest that the reactions
362 comprise a specific pathway for the detoxification of structurally related plant alkaloids. AQ
363 transformation might even represent a natural “biocontrol pathway”, enabling strain BG43 to
364 interfere with AQ-dependent quorum sensing systems. In this context, it is interesting that among
365 the isolates from the soil sample that yielded strain BG43, two were tentatively assigned to the

Downloaded from http://aem.asm.org/ on October 17, 2017 by guest

AEM Accepts published online ahead of print

Downloaded from http://aem.asm.org/ on October 17, 2017 by guest

366 species *P. aeruginosa,* based on partial 16S rRNA sequences and their ability to synthesize PQS
367 (data not shown), indicating that *Rhodococcus* sp. and *P. aeruginosa* coexisted in this sample.
368 The identification of the *qsdA* gene in strain BG43, which codes for an AHL lactonase active
369 against a broad range of AHL signal molecules (21, 46, 51), suggests that strain BG43 can also
370 disrupt AHL-based communication, like other *Rhodococcus* strains that contain *qsdA* (21, 23).

371 Remarkably, *Rhodococcus* sp. BG43 was observed to slowly convert the respiratory
372 inhibitor HQNO to PQS. Thus, *Rhodococcus* sp. BG43 transforms a secondary metabolite of *P.*
373 *aeruginosa* with antibiotic activity to a *Pseudomonas* QS signal molecule (Fig. 6). Considering
374 the comparatively fast elimination of PQS added to cell suspensions of strain BG43, it is
375 interesting to note that PQS formed intracellularly from HQNO slowly accumulated to up to
376 several µM (compare Figs. 2A and 4A). The molecular basis of this effect is not yet known,
377 however, based on the kinetics of anthranilate formation from PQS by HQNO-treated cell
378 extracts, we can exclude the possibility that HQNO or hydroxy-HQNO act as inhibitor of the
379 PQS-converting enzyme.

380 The observation of transient formation of HHQ as well as the identification of PQS in the
381 HQNO bioconversion assays suggest that strain BG43 has an *N*-oxide reductase. While reduction
382 of several organic *N*-oxides by gut bacteria has been described (52, 53), we are not aware of a
383 report on reduction of 2-alkyl-4-hydroxyquinoline-*N*-oxides by axenic cultures of aerobic or
384 anaerobic bacteria. In mammalians, enzymatic reduction of aromatic *N*-oxides such as
385 quinoxaline-1,4-dioxides, which are used as drugs and animal feed additives, is catalyzed by liver
386 aldehyde oxidase and xanthine oxidoreductase (54–56). Recently, the mitochondrial amidoxime
387 reducing component 1 (mARC1), another mammalian molybdenum enzyme, was reported to
388 catalyze the reduction of nicotinamide-*N*-oxide in the presence of cytochrome b_5 and NADH-
389 cytochrome b_5 reductase (57).

AEM Accepts published online ahead of print

390 The isolation of *Rhodococcus* sp. BG43 and the identification of reactions for the
391 degradation of AQ-type quorum sensing signaling molecules and for *N*-oxide reduction of the
392 antibacterial compound HQNO opens up interesting new perspectives for studying bacterial inter-
393 species interactions, for the biochemical characterization of novel quorum quenching and
394 detoxification enzymes, and for the development of therapeutic agents that target AQ signaling.
395

396 **Acknowledgements**

397 We thank Stephan Heeb (Nottingham, UK) for kindly providing the pME6032 vector, and Eliza
398 Yeh-Chen Soh and Paul Williams (Nottingham, UK) for sharing methods prior to publication.
399 We also thank Björn Fischer (Münster, Germany) for setting up enrichment cultures, and Bodo
400 Philipp and Onur Yücel (Münster, Germany) for access to the mass spectrometer and help with
401 MS analyses. Acquisition of the mass spectrometer was supported by the Deutsche
402 Forschungsgemeinschaft (INST 211/646-1). This work was supported by the Deutsche
403 Forschungsgemeinschaft in the framework of the Graduate School GRK1409 'Molecular
404 Interactions of Pathogens with Biotic and Abiotic Surfaces'.
405

406 ***References***

407 1. **Williams P, Winzer K, Chan WC, Cámara M. 2007.** Look who's talking:
408 communication and quorum sensing in the bacterial world. Philos. Trans. R. Soc. London
409 Ser. B **362:**1119–1134.

410 2. **Heeb S, Fletcher MP, Chhabra SR, Diggle SP, Williams P, Cámara M.** 2011.
411 Quinolones: from antibiotics to autoinducers. FEMS Microbiol. Rev. **35:**247–274.

Downloaded from http://aem.asm.org/ on October 17, 2017 by guest

AEM Accepts published online ahead of print

412 3. **Huse H, Whiteley M.** 2011. 4-Quinolones: smart phones of the microbial world. Chem.
413 Rev. **111:**152–159.
414 4. **Nadal Jimenez P, Koch G, Thompson JA, Xavier KB, Cool RH, Quax WJ.** 2012. The
415 multiple signaling systems regulating virulence in *Pseudomonas aeruginosa*. Microbiol.
416 Mol. Biol. Rev. **76:**46–65.
417 5. **Debitus C, Guella G, Mancini I, Waikedre J, Guemas JP, Nicolas JL, Pietra F**. 1998
418 Quinolones from a bacterium and tyrosine metabolites from its host sponge, *Suberea*
419 *creba* from the Coral Sea. J. Mar. Biotechnol. **6:**136–141.
420 6. **Long RA, Qureshi A, Faulkner DJ, Azam F.** 2003. 2-*n*-Pentyl-4-quinolinol produced
421 by a marine *Alteromonas* sp. and its potential ecological and biogeochemical roles. Appl.
422 Environ. Microbiol. **69:**568–576.
423 7. **Diggle SP, Lumjiaktase P, Dipilato F, Winzer K, Kunakorn M, Barrett DA,**
424 **Chhabra SR, Cámara M, Williams P.** 2006. Functional genetic analysis reveals a 2-
425 alkyl-4-quinolone signaling system in the human pathogen *Burkholderia pseudomallei*
426 and related bacteria. Chem. Biol. **13:**701–710.
427 8. **Vial L, Lépine F, Milot S, Groleau MC, Dekimpe V, Woods DE, Déziel E.** 2008.
428 *Burkholderia pseudomallei*, *B. thailandensis*, and *B. ambifaria* produce 4-hydroxy-2-
429 alkylquinoline analogues with a methyl group at the 3 position that is required for
430 quorum-sensing regulation. J. Bacteriol. **190:**5339–5352.
431 9. **Lépine F, Milot S, Déziel E, He J, Rahme LG.** 2004. Electrospray/mass spectrometric
432 identification and analysis of 4-hydroxy-2-alkylquinolines (HAQs) produced by
433 *Pseudomonas aeruginosa*. J. Am. Soc. Mass Spectrom. **15:**862–869.

Downloaded from http://aem.asm.org/ on October 17, 2017 by guest

AEM Accepts published online ahead of print

434 10. **Lightbown JW, Jackson FL.** 1956. Inhibition of cytochrome systems of heart muscle
435 and certain bacteria by the antagonists of dihydrostreptomycin: 2-alkyl-4-
436 hydroxyquinoline *N*-oxides. Biochem. J. **63:**130–137.

437 11. **Gao X, Wen X, Esser L, Quinn B, Yu L, Yu C-A, Xia D.** 2003. Structural basis for the
438 quinone reduction in the bc_1 complex: a comparative analysis of crystal structures of
439 mitochondrial cytochrome bc_1 with bound substrate and inhibitors at the Q_i site.
440 Biochemistry **42:**9067–9080.

441 12. **O'Connell KMG, Hodgkinson JT, Sore HF, Welch M, Salmond GPC, Spring DR.**
442 2013. Combating multidrug-resistant bacteria: current strategies for the discovery of novel
443 antimicrobials. Angew. Chem. Int. Ed. **52:**10706–10733.

444 13. **Defoirdt T, Boon N, Bossier P.** 2010. Can bacteria evolve resistance to quorum sensing
445 disruption? PLoS Pathog. **6(7)**:e1000989. doi: 10.1371/journal.ppat.1000989.

446 14. **Garcìa-Contreras R, Maeda T, Wood TK.** 2013. Resistance to quorum-quenching
447 compounds. Appl. Environ. Microbiol. **79:**6840–6846.

448 15. **LaSarre B, Federle MJ.** 2013. Exploiting quorum sensing to confuse bacterial
449 pathogens. Microbiol. Mol. Biol. Rev. **77:**73–111.

450 16. **Du Y, Li T, Wan Y, Liao P.** 2014. Signal molecule-dependent quorum-sensing and
451 quorum-quenching enzymes in bacteria. Crit. Rev. Eukaryot. Gene Expr. **24:**117–132.

452 17. **Leblanc JC, Gonçalves ER, Mohn WW.** 2008. Global response to desiccation stress in
453 the soil actinomycete *Rhodococcus jostii* RHA1. Appl. Environ. Microbiol. **74:**2627–
454 2636.

455 18. **Fanget NVJ, Foley S.** 2011. Starvation/stationary-phase survival of *Rhodococcus*
456 *erythropolis* SQ1: a physiological and genetic analysis. Arch. Microbiol. **193:**1–13.

Downloaded from http://aem.asm.org/ on October 17, 2017 by guest

457 19. **Larkin MJ, Kulakov LA, Allen CCR.** 2005. Biodegradation and *Rhodococcus* – masters
458 of catabolic versatility. Curr. Opin. Biotechnol. **16:**282–290.
459 20. **Larkin MJ, Kulakov LA, Allen CCR.** 2006. Biodegradation by members of the genus
460 *Rhodococcus*: biochemistry, physiology, and genetic adaptation. Adv. Appl. Microbiol.
461 **59:**1–29.
462 21. **Uroz S, Oger PM, Chapelle E, Adeline MT, Faure D, Dessaux Y.** 2008. A
463 *Rhodococcus qsdA*-encoded enzyme defines a novel class of large-spectrum quorum-
464 quenching lactonases. Appl. Environ. Microbiol. **74:**1357–1366.
465 22. **Barbey C, Crépin A, Cirou A, Budin-Verneuil A, Orange N, Feuilloley M, Faure D,**
466 **Dessaux Y, Burini JF, Latour X.** 2012. Catabolic pathway of gamma-caprolactone in
467 the biocontrol agent *Rhodococcus erythropolis*. J. Proteome Res. **11:**206–216.
468 23. **Barbey C, Crépin A, Bergeau D, Ouchiha A, Mijouin L, Taupin L, Orange N,**
469 **Feuilloley M, Dufour A, Burini JF, Latour X.** 2013. *In planta* biocontrol of
470 *Pectobacterium atrosepticum* by *Rhodococcus erythropolis* involves silencing of
471 pathogen communication by the rhodococcal gamma-lactone catabolic pathway. PLoS
472 ONE **8(6):**e66642. doi: 10.1371/journal.pone.0066642.
473 24. **Uroz S, D'Angelo-Picard C, Carlier A, Elasri M, Sicot C, Petit A, Oger P, Faure D,**
474 **Dessaux Y.** 2003. Novel bacteria degrading *N*-acylhomoserine lactones and their use as
475 quenchers of quorum-sensing-regulated functions of plant-pathogenic bacteria.
476 Microbiology **149:**1981–1898.
477 25. **Cirou A, Raffoux A, Diallo S, Latour X, Dessaux Y, Faure D.** 2011. Gamma-
478 caprolactone stimulates growth of quorum-quenching *Rhodococcus* populations in a
479 large-scale hydroponic system for culturing *Solanum tuberosum*. Res. Microbiol.
480 **162:**945–950.

AEM Accepts published online ahead of print

Downloaded from http://aem.asm.org/ on October 17, 2017 by guest

AEM Accepts published online ahead of print

481 26. **Pustelny C, Albers A, Büldt-Karentzopoulos K, Parschat K, Chhabra SR, Cámara**
482 **M, Williams P, Fetzner S.** 2009. Dioxygenase-mediated quenching of quinolone-
483 dependent quorum sensing in *Pseudomonas aeruginosa*. Chem. Biol. **16:**1259–1267.
484 27. **Niewerth H, Schuldes J, Parschat K, Kiefer P, Vorholt JA, Daniel R, Fetzner S.**
485 2012. Complete genome sequence and metabolic potential of the quinaldine-degrading
486 bacterium *Arthrobacter* sp. Rue61a. BMC Genomics **13:**534. doi: 10.1186/1471-2164-13-
487 534.
488 28. **Thierbach S, Bui N, Zapp J, Chhabra SR, Kappl R, Fetzner S.** 2014. Substrate-
489 assisted O_2 activation in a cofactor-independent dioxygenase. Chem. Biol. **21:**217–225.
490 29. **Oliva A, Meepegala KM, Wedge DE, Harries D, Hale AL, Aliotta G, Duke SO.** 2003.
491 Natural fungicides from *Ruta graveolens* L. leaves, including a new quinolone alkaloid. J.
492 Agric. Food Chem. **51:**890–896.
493 30. **Michael JP.** 2008. Quinoline, quinazoline and acridone alkaloids. Nat. Prod. Rep.
494 **25:**166–187.
495 31. **Niewerth H, Bergander K, Chhabra SR, Williams P, Fetzner S.** 2011. Synthesis and
496 biotransformation of 2-alkyl-4(1*H*)-quinolones by recombinant *Pseudomonas putida*
497 KT2440. Appl. Microbiol. Biotechnol. **91:**1399–1408.
498 32. **Cornforth JW, James AT.** 1956. Structure of a naturally occurring antagonist of
499 dihydrostreptomycin. Biochem. J. **63:**124–130.
500 33. **Eiden F, Wendt R, Fenner H.** 1978. Pyrones and pyridones. 74. Quinolylidene
501 derivatives. Arch. Pharm. (Weinheim, Ger.) **311:**561–568.
502 34. **Bauder R, Tshisuaka B, Lingens F.** 1990. Microbial metabolism of quinoline and
503 related compounds. VII. Quinoline oxidoreductase from *Pseudomonas putida*: a
504 molybdenum-containing enzyme. Biol. Chem. Hoppe Seyler. **371:**1137–1144.

Downloaded from http://aem.asm.org/ on October 17, 2017 by guest

AEM Accepts published online ahead of print

505 35. **Sambrook J, Fritsch EF, Maniatis T.** 1989. Molecular Cloning: a Laboratory Manual,
506 2nd ed. Cold Spring Harbor Laboratory, Cold Spring Harbor, NY.
507 36. **Chan KG, Yin WF, Sam CK, Koh CL.** 2009. A novel medium for the isolation of *N*-
508 acylhomoserine lactone-degrading bacteria. J. Ind. Microbiol. Biotechnol. **36:**247–251.
509 37. **Parschat K, Overhage J, Strittmatter AW, Henne A, Gottschalk G, Fetzner S.** 2007.
510 Complete nucleotide sequence of the 113-kilobase linear catabolic plasmid pAL1 of
511 *Arthrobacter nitroguajacolicus* Rü61a and transcriptional analysis of genes involved in
512 quinaldine degradation. J. Bacteriol. **189:**3855–3867.
513 38. **Hanahan D.** 1983. Studies on transformation of *Escherichia coli* with plasmids. J. Mol.
514 Biol. **166:**557–580.
515 39. **Iwasaki K, Uchiyama H, Yagi O, Kurabayashi T, Ishizuka K, Takamura Y.** 1994.
516 Transformation of *Pseudomonas putida* by electroporation. Biosci. Biotechnol. Biochem.
517 **58:**851–854.
518 40. **Heeb S, Itoh Y, Nishijyo T, Schnider U, Keel C, Wade J, Walsh U, O'Gara F, Haas**
519 **D.** 2000. Small, stable shuttle vectors based on the minimal pVS1 replicon for use in
520 Gram-negative, plant-associated bacteria. Mol. Plant Microbe Interact. **13:**232–237.
521 41. **Weisburg WG, Barns SM, Pelletier DA, Lane DJ.** 1991. 16S ribosomal DNA
522 amplification for phylogenetic study. J. Bacteriol. **173:**697–703.
523 42. **Muyzer G, Teske A, Wirsen CO, Jannasch HW.** 1995. Phylogenetic relationships of
524 *Thiomicrospira* species and their identification in deep-sea hydrothermal vent samples by
525 denaturing gradient gel electrophoresis of 16S rDNA fragments. Arch. Microbiol.
526 **164:**165–172.
527 43. **Táncsics A, Benedek T, Farkas M, Máthé I, Márialigeti K, Szoboszlay S, Kukolya J,**
528 **Kriszt B.** 2014. Sequence analysis of 16S rRNA, *gyrB* and *catA* genes and DNA-DNA

Downloaded from http://aem.asm.org/ on October 17, 2017 by guest

529 hybridization reveal that *Rhodococcus jialingiae* is a later synonym of *Rhodococcus*
530 *qingshengii*. Int. J. Syst. Evol. Microbiol. **64:**298–301.
531 44. **Tamura K, Stecher G, Peterson D, Filipski A, Kumar S.** 2013. MEGA6: Molecular
532 evolutionary genetics analysis version 6.0. Mol. Biol. Evol. **30:**2725–2729.
533 45. **Edgar RC.** 2004. MUSCLE: a multiple sequence alignment method with reduced time
534 and space complexity. BMC Bioinformatics **5:**113. doi:10.1186/1471-2105-5-113.
535 46. **Oh HS, Kim SR, Cheong WS, Lee CH, Lee JK.** 2013. Biofouling inhibition in MBR by
536 *Rhodococcus* sp. BH4 isolated from real MBR plant. Appl. Microbiol. Biotechnol.
537 **97:**10223–10231.
538 47. **Zor T, Selinger Z.** 1996. Linearization of the Bradford protein assay increases its
539 sensitivity: theoretical and experimental studies. Anal. Biochem. **236:**302–308.
540 48. **Xu JL, He J, Wang ZC, Wang K, Li WJ, Tang SK, Li SP.** 2007. *Rhodococcus*
541 *qingshengii* sp. nov., a carbendazim-degrading bacterium. Int. J. Syst. Evol. Microbiol.
542 **57**:2754–2757.
543 49. **Wang Z, Xu J, Li Y, Wang K, Wang Y, Hong Q, Li WJ, Li SP.** 2010. *Rhodococcus*
544 *jialingiae* sp. nov., an actinobacterium isolated from sludge of a carbendazim wastewater
545 treatment facility. Int. J. Syst. Evol. Microbiol. **60:**378–381.
546 50. **Schertzer JW, Brown SA, Whiteley M.** 2010. Oxygen levels rapidly modulate
547 *Pseudomonas aeruginosa* social behaviours via substrate limitation of PqsH. Mol.
548 Microbiol. **77:**1527–1538.
549 51. **Afriat L, Roodveldt C, Manco G, Tawfik DS.** 2006. The latent promiscuity of newly
550 identified microbial lactonases is linked to a recently diverged phosphotriesterase.
551 Biochemistry **45:**13677−13686.

AEM Accepts published online ahead of print

Downloaded from http://aem.asm.org/ on October 17, 2017 by guest

AEM Accepts published online ahead of print

552 52. **Jenner P, Gorrod JW, Beckett AH.** 1973. The absorption of nicotine-1'-*N*-oxide and its
553 reduction in the gastro-intestinal tract in man. Xenobiotica **3:**341−349.
554 53. **Li Y, Xu J, Lai WG, Whitcher-Johnstone A, Tweedie DJ.** 2012. Metabolic switching
555 of BILR 355 in the presence of Ritonavir. II. Uncovering novel contributions by gut
556 bacteria and aldehyde oxidase. Drug Metab. Dispos. **40:**1130−1137.
557 54. **Kitamura S, Sugihara K, Ohta S.** 2006. Drug-metabolizing ability of molybdenum
558 hydroxylases. Drug Metab. Pharmacokinet. **21:**83−98.
559 55. **Mu P, Zheng M, Xu M, Zheng Y, Tang X, Wang Y, Wu K, Chen Q, Wang L, Deng
560 Y.** 2014. *N*-Oxide reduction of quinoxaline-1,4-dioxides catalyzed by porcine aldehyde
561 oxidase SsAOX1. Drug Metab. Dispos. **42:**511−519.
562 56. **Chen C, Cheng G, Hao H, Dai M, Wang X, Huang L, Liu Z, Yuan Z.** 2013.
563 Mechanism of porcine liver xanthine oxidoreductase mediated *N*-oxide reduction of
564 Cyadox as revealed by docking and mutagenesis studies. PLoS ONE **8(9):**e73912. doi:
565 10.1371/journal.pone.0073912.
566 57. **Jakobs HH, Froriep D, Havemeyer A, Mendel RR, Bittner F, Clement B**. 2014. The
567 mitochondrial amidoxime reducing component (mARC): involvement in metabolic
568 reduction of *N*-oxides, oximes and *N*-hydroxyamidinohydrazones. ChemMedChem, doi:
569 10.1002/cmdc.201402127. [Epub ahead of print].
570

Downloaded from http://aem.asm.org/ on October 17, 2017 by guest

AEM Accepts published online ahead of print

Downloaded from http://aem.asm.org/ on October 17, 2017 by guest

571 **Figure legends**

572 **Fig. 1**: Phylogenetic trees based on marker genes of *Rhodococcus* sp. BG43 and closely
573 related type strains. **A**: 16S rRNA gene, **B**: *gyrB*, **C**: *catA,* **D**: joined *catA*-*gyrB*-16S rRNA
574 genes. Trees were constructed with Molecular Evolution Genetic Analysis (MEGA) software
575 version 6.0 using the neighbor-joining algorithm (44). Nucleotide alignment was performed
576 with MUSCLE (45). The reliability of the trees was evaluated with bootstrap analysis (1000
577 resamplings).

578

579 **Fig. 2**: Cometabolic conversion of AQs by *Rhodococcus* sp. BG43. Cell suspensions of
580 *Rhodococcus* sp. BG43 (OD_{600nm} ~ 3) were incubated in modified KG medium with succinate
581 and 20 µM PQS (**A**) or HHQ (**B**). The first culture sample was withdrawn and mixed with
582 acidified ethyl acetate 3 min after AQ addition to the cells. The culture samples were
583 extracted with ethyl acetate, and AQs and anthranilic acid in the extracts were quantified by
584 HPLC. Squares: PQS; circles: anthranilic acid; triangles: HHQ. Filled symbols indicate
585 substrates added to cultures, open symbols indicate intermediates or products formed. Data
586 represent mean values from three independent biological replicates ± standard deviations. **C**:
587 HPLC elution profiles of the conversion of an AQ preparation that besides HHQ (major peak
588 at retention time 39.1 min) additionally contains the *trans* and *cis* isomer of unsaturated HHQ
589 ($C_{7:1}$; at 37.9 min and 38.7 min, respectively), as well as long-chain AQs (C_8-, C_9-, C_{11}-, C_{13}-
590 AQ at 41.3, 43.2, 46.0 and 47.0 min) and the *cis*/*trans* isomers of their unsaturated congeners
591 ($C_{9:1}$, $C_{11:1}$, $C_{13:1}$; *trans* isomers have shorter retention times than the corresponding *cis*
592 isomers (31)). PQS elutes at 40.2 min (90 min trace).

593

AEM Accepts published online ahead of print

594 **Fig. 3**: Rates of AQ conversion by cell extracts of *Rhodococcus* sp. BG43 (µM AQ converted
595 per hour and mg total protein). Desalted crude cell extracts (2 mg protein/ml) were incubated
596 with 20 µM HHQ and 500 µM NADH, or with 20 µM PQS. White bars represent extracts
597 from cells grown in LB, gray bars represent extracts from LB cultures supplemented with
598 PQS 2 hours prior to harvesting. Data represent mean values from two independent biological
599 replicates ± standard error. Cell extracts treated for 10 min at 99 °C did not support AQ
600 conversion.
601
602 **Fig. 4**: Conversion of HQNO by *Rhodococcus* sp. BG43. **A**: Cell suspensions of
603 *Rhodococcus* sp. BG43 (OD_{600nm} ~ 3) were incubated in modified KG medium with succinate
604 and 20 µM HQNO. AQs in ethyl acetate extracts of culture samples were quantified by
605 HPLC. Diamonds: HQNO, squares: PQS; up-pointing triangles: HHQ; down-pointing
606 triangles: metabolite identified as a hydroxylated form of HQNO, detected at 350 nm. Filled
607 symbols indicate substrate added to cultures, open symbols indicate intermediates or products
608 formed. Data represent mean values from three independent biological replicates ± standard
609 deviations. **B**: UV absorption spectra (HPLC-diode array detection) of HQNO and the
610 metabolites formed. Spectra of HQNO, PQS, and hydroxy-HQNO are represented by dashed,
611 continuous, and dotted lines, respectively. The inset shows the corresponding HPLC elution
612 profiles of ethyl acetate extracts of culture samples, extracted after 5 min (dotted line) and
613 after 24 hours (continuous line). Peaks represent PQS (retention time 10.1 min), HQNO (at
614 10.8 min), and hydroxy-HQNO (at 11.8 min).
615
616 **Fig. 5**: Anthranilic acid formation from PQS by HQNO-treated crude cell extracts. Desalted
617 crude cell extracts (1 mg protein/ml) of PQS-induced cells were pre-incubated with 500 µM

Downloaded from http://aem.asm.org/ on October 17, 2017 by guest

AEM Accepts published online ahead of print

618 NADH and 0, 20 or 50 µM of HQNO for 30 min, and subsequently (at t=0 min) 20 µM of
619 PQS was added. Samples were extracted with ethyl acetate, and HQNO (open symbols) and
620 anthranilic acid (filled symbols) were quantified by HPLC. Squares, circles and triangles
621 represent samples from crude extracts pre-incubated with 0, 20 µM, and 50 µM of HQNO,
622 respectively. Data are mean values from two independent experiments.
623
624 **Fig. 6**: Proposed pathways of HHQ, PQS and HQNO conversion by *Rhodococcus* sp. BG43.
625

Downloaded from http://aem.asm.org/ on October 17, 2017 by guest

626 **Table 1**: Primers used in this study.

Primer designation	Sequence 5'→3'	Application	Reference
pqsL-for	ATATGAGCTCTCA*G*TGGTGGT GGTGGTGGTGGCCGAGCGGC GCCGGCGACCGCACCGGCTG	Amplification of *pqsL* (nt 4687652-4688848 of *P. aeruginosa* PAO1)	This study
pqsL-rev	ATATGAATTCATGACGGACAA CCATATCGATGTACTGATC		
GM3F	AGAGTTTGATC(AC)TGGC	Amplification of 16S rRNA gene	41, 42
GM4R	TACCTTGTTACGACTT		
catA-for	GCCGCCACCGACAAGTT	Amplification of catechol 1,2-dioxygenase gene *catA*	43
catA-rev	CACCATGAGGTGCAGGTG		
gyrB-for	GGCGGCAAGTTCGACTTCGA	Amplification of gyrase B gene *gyrB*	43
gyrB-rev	GCCTTCTCGACGTTGATGATC		
qsdA-for	ATGAGTTCAGTACAAACCGT	Amplification of AHL lactonase gene *qsdA*	46
qsdA-rev	TCAGCTCTCGAAGTACCGAC		

627

AEM Accepts published online ahead of print

Downloaded from http://aem.asm.org/ on October 17, 2017 by guest

AEM Accepts published online ahead of print

628 **Table 2**: Growth of *Rhodococcus* sp. BG43 and closely related type strains on selected
629 carbon sources. Data for the type strains are from references (48, 49). Strain BG43 was
630 cultured in modified KG medium with shaking at 30 °C. D-fructose, lactose, glycerol, D-
631 mannose, D-xylose or *myo*-inositol: 2% (wt/vol); sucrose: 4 mM; D-sorbitol: 1% (wt/vol);
632 catechol: 1%, 0.5% or 0.1% (wt/vol). OD_{600nm} was measured after 24 hours of incubation.
633 +: $OD_{600nm} > 0.5$; w: weak, $OD_{600nm} < 0.5$; −: no growth observed.

Carbon source	***Rhodococcus* sp. BG43**	***R. erythropolis* DSM 43066^T**	***R. baikonurensis* DSM 44587^T**	***R. qingshengii* DSM 45222^T**	***R. globerulus* DSM 43954^T**
D-Fructose	+	+	+	−	+
Sucrose	+	+	−	w	+
D-Sorbitol	+	+	−[a]/ +[b]	−	+
Catechol	−	−	−	+	−
Lactose	−	−	−	−	−
Glycerol	+	+	+	+	+
D-Mannose	w	−	w	+	+
D-Xylose	w	−	−	−	+
myo-Inositol	+	+	−	−	−

634

635 [a] (48); [b] (49)

Downloaded from http://aem.asm.org/ on October 17, 2017 by guest

AEM Accepts published online ahead of print

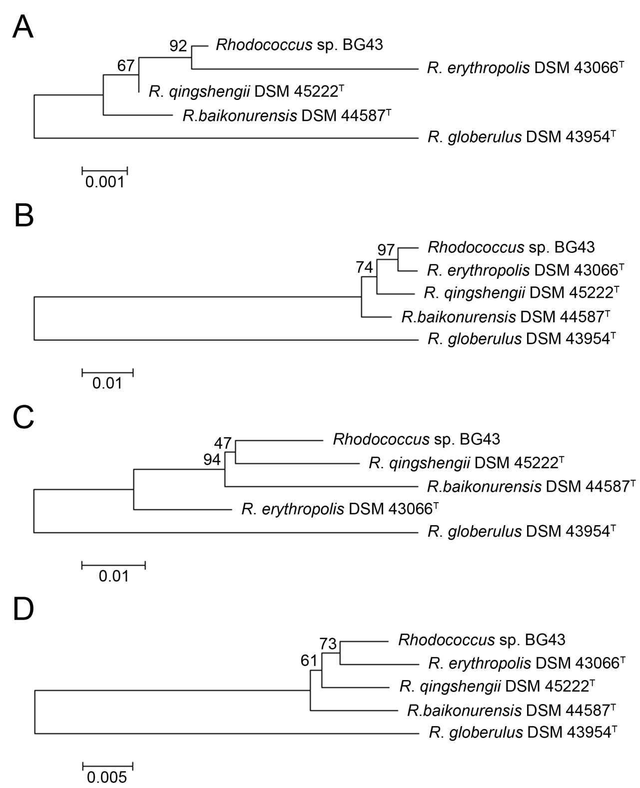

Downloaded from http://aem.asm.org/ on October 17, 2017 by guest

AEM Accepts published online ahead of print

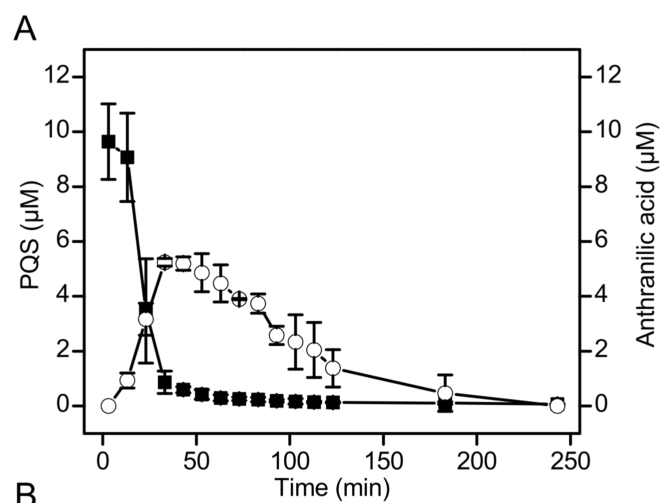

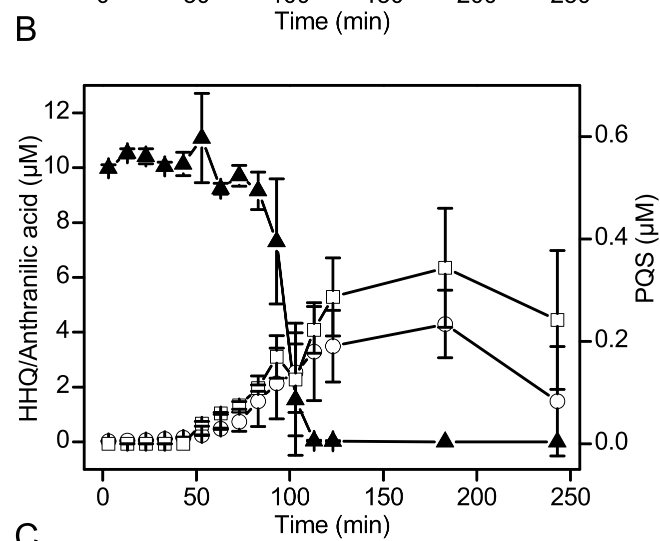

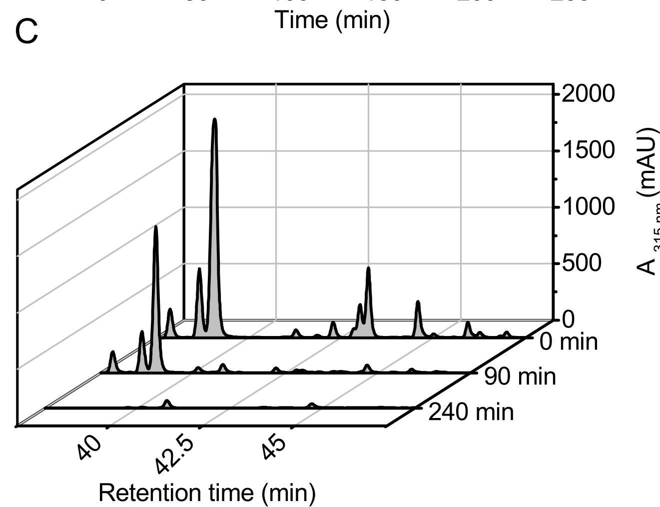

Downloaded from http://aem.asm.org/ on October 17, 2017 by guest

AEM Accepts published online ahead of print

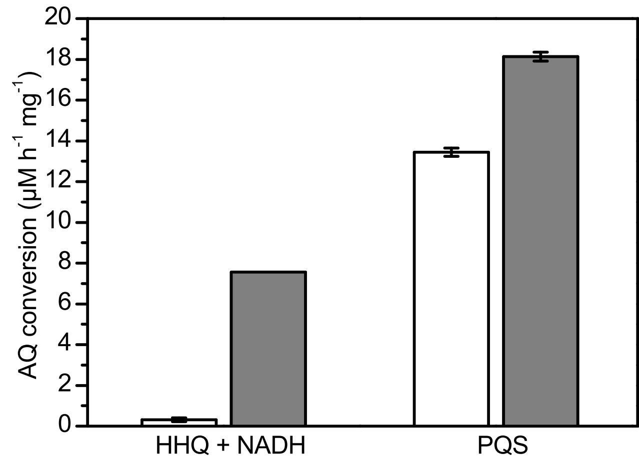

Downloaded from http://aem.asm.org/ on October 17, 2017 by guest

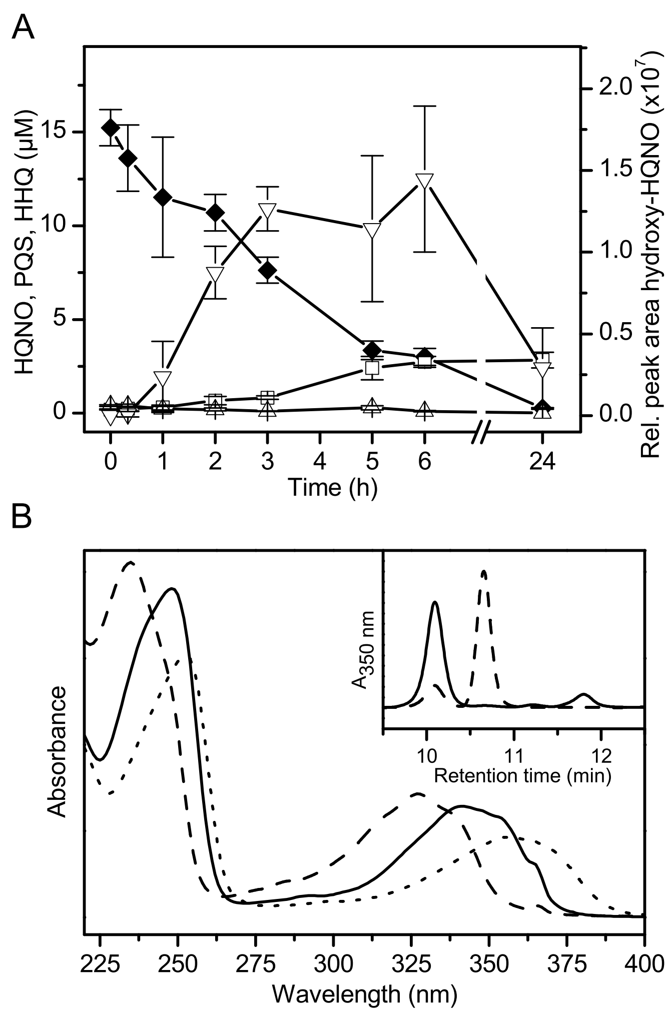

AEM Accepts published online ahead of print

Downloaded from http://aem.asm.org/ on October 17, 2017 by guest

AEM Accepts published online ahead of print

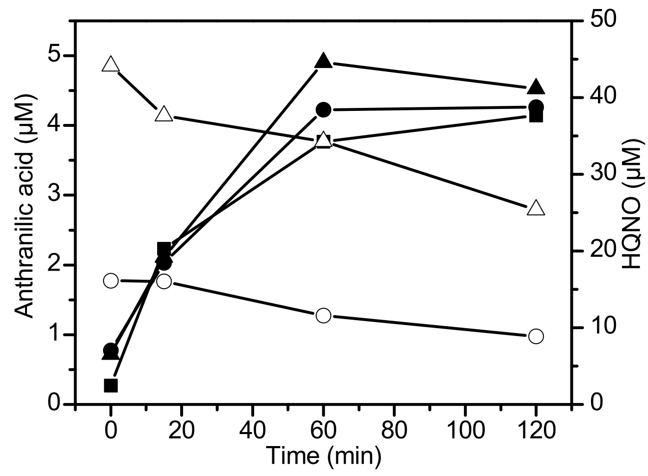

Downloaded from http://aem.asm.org/ on October 17, 2017 by guest

AEM Accepts published online ahead of print

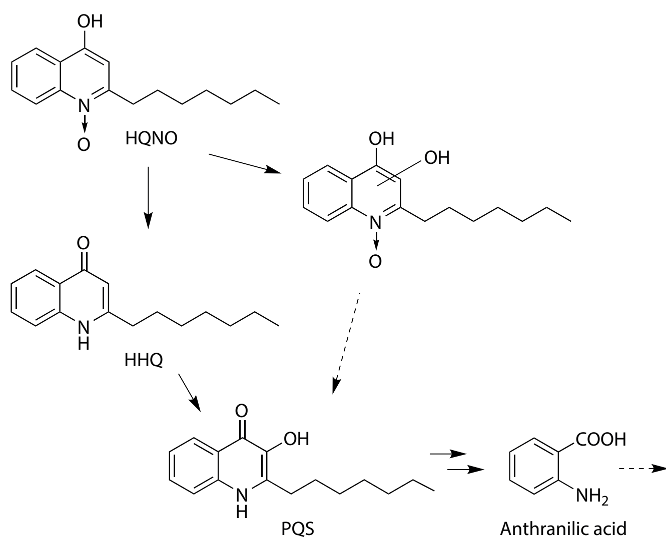

Downloaded from http://aem.asm.org/ on October 17, 2017 by guest